Host-structure-dependent non-Lorentzian persistent-hole shapes in organic glasses

Sadao Uemura,* Masashi Okada, Akihito Wakamiya, and Hiroki Nakatsuka
Institute of Applied Physics, University of Tsukuba, Tsukuba, Ibaraki 305, Japan
(Received 13 May 1992)

Nonexponential photon-echo decay curves and non-Lorentzian persistent-hole shapes of chromophores in organic glasses have been observed experimentally, and explained by considering fractal structures of the organic-glass hosts. The photon-echo decay curves are well reproduced by the nonexponentially decaying function of τ, $\exp(-cT\tau^{D/3})$, where c is a constant, T is the temperature, τ is the delay time between the first and second excitation pulses, and D is the fractal dimension of the glass host. The persistent-hole shapes are also well reproduced by the Fourier transform of this function. The fractal dimensions D obtained by fitting the theoretical curves to the observed hole shapes were characteristic of the hosts, and almost independent of the guest chromophore. The non-Lorentzian persistent-hole shapes were observed in nonionic as well as in ionic guest chromophores. We also obtained consistent values of the host fractal dimension from the photon-echo decay curves. A simple model of glass structure is presented which can consistently explain the differences between polymeric glass host and monomeric glass host with regard to the measured hole shapes, echo decay curves, and the interrelations between the hole widths and the inhomogeneous widths.

I. INTRODUCTION

In 1971, Zeller and Pohl found out that thermal conductivity and heat capacity of several glasses show behaviors differing very much from those of their crystalline counterparts.[1] It is now well established that various physical properties in amorphous materials are very different from those of crystalline materials at low temperatures. Anderson, Halperin, and Varma[2] and Phillips[3] independently proposed a model based on two-level systems (TLS's) which could explain these differences. In 1974 Kharlamov, Personov, and Bykovskaya[4] and Gorokhovskii, Kaarli, and Rebane[5] discovered the burning of persistent holes in the inhomogeneously broadened absorption bands of organic molecules embedded in low-temperature amorphous matrices. The importance of the TLS concept in persistent-hole burning (PHB) was first pointed out by Small and Hayes,[6,7] and since then there have been many theoretical works on the persistent-hole width and its temperature dependence based on the TLS model.[7-14]

Recently we[15-17] observed the persistent holes in some ionic-dye-doped organic glasses, and found out that, although the persistent-hole shapes in a monomeric glass host are close to Lorentzian, those in a long-chain polymeric glass host deviate significantly from Lorentzian shapes.

It is well known that hole shapes and photon-echo decay curves are related by a Fourier transformation.[18-20] Hu and Walker analyzed the dephasing and the spectral diffusion of spin systems by random spin floppings.[21] If we consider the spin floppings as jumps in the TLS's, their analysis can be applied to amorphous systems. Maynard, Rammal, and Suchail[22] and Bai and Fayer[23] discussed the photon-echo decay curves by assuming that the spatial distribution of the TLS's is uniform and that the interaction between the TLS and the guest chromophore is of dipole-dipole type. Under these assumptions they derived the single-exponential photon-echo decay curve which corresponds to the Lorentzian hole shape. However, non-Lorentzian persistent-hole shapes have also been obtained by considering other types of interactions between the chromophore and the TLS.[24] Experimentally we found different persistent-hole shapes for a guest chromophore between a polymeric glass host, polyvinyl alcohol (PVA), and a monomeric glass host, ethanol (EtOH). Since EtOH is the basic component of PVA, the type of interaction between the TLS and the guest chromophore should be the same for both of the glass hosts. Therefore, the difference of the hole shapes between PVA and EtOH cannot be solely attributed to the difference in the interaction between the TLS and the guest chromophore.

It has been pointed out that polymer chains in organic glasses form fractal structures.[25,26] Alexander and Orbach[27] have developed the fracton model based on the fractal concept to describe the anomalous vibration properties of glasses. Saikan *et al.*[28] discussed the relation between Raman-scattering spectra in polymeric glasses and phonon side band spectra in persistent holes in terms of fracton modes. If TLS's are on the polymer chains, the spatial distribution of the TLS's themselves should also form a fractal structure. By assuming that the TLS's in the polymer host are spatially distributed like a fractal with a fractal dimension D and that the TLS's in the phonon bath interact with the guest chromophore via dipole-dipole interaction, we have derived a nonexponential photon-echo decay curve and a non-Lorentzian persistent-hole shape. In this paper, we present the simple and self-contained theory.

In order to verify our theory, we measured the hole shapes and the photon-echo decay curves in some organic

glasses, and obtained the non-Lorentzian hole shapes and the nonexponentially decaying photon-echo decay curves. The values of fractal dimensions D derived from these curves were in good qualitative agreement with our simple model for the spatial structures of the glass hosts.

II. THEORY

It is known that the photon-echo decay curve in the time-domain and the hole shape in the frequency domain are related by a Fourier transformation.[18–20] The hole shape $I_H(\omega)$ is given by the Fourier transform of the four-point correlation function or the stimulated photon-echo decay function $C(\tau,T_w,\tau)$ introduced by Berg *et al.*,[18]

$$I_H(\omega)\propto\int_{-\infty}^{\infty}d\tau\exp(i\omega\tau)C(\tau,T_w,\tau)\ , \tag{1}$$

where τ and T_w are the intervals between the first and second pulses, and the second and third pulses of the stimulated photon echo, respectively. In the stimulated photon echo, τ changes in the order of the dephasing time T_2, while T_w can be as long as the population grating decay time T_1 which is practically infinite for PHB materials. In hole-burning spectroscopy, T_w in Eq. (1) corresponds to the waiting time between burn and probe.

At very low temperatures the dephasing of the chromophore in organic glasses is caused mainly by the TLS's. If we assume that the decay of the stimulated photon echo is caused by the TLS's, the echo decay function $C(\tau,T_w,\tau)$ can be expressed as

$$C(\tau,T_w,\tau)=\left\langle\exp\left[i\sum_j^N\phi_j(\tau,T_w)\right]\right\rangle_{H,\mathrm{TLS}}\ , \tag{2}$$

where $\langle\ \rangle_{H,\mathrm{TLS}}$ represents the averages over the history path and the parameters of the TLS, N is the number of TLS's surrounding the chromophore, and ϕ_j is the phase shift of the chromophore caused by the jump of the jth TLS which can be expressed as

$$\phi_j(\tau,T_w)=\Delta\omega_j\left[\int_0^{\tau}h(t)dt-\int_{T_w+\tau}^{T_w+2\tau}h(t)dt\right]\ , \tag{3}$$

where $h(t)$ takes the values $+1$ or -1 randomly, and is called the random telegraph function.[23] If there is no correlation between different TLS's, Eq. (2) becomes

$$\begin{aligned}C(\tau,T_w,\tau)&=\prod_{j=1}^{N}\langle\exp[i\phi_j(\tau,T_w,\tau)]\rangle_{H,\mathrm{TLS}}\\&=\langle\exp[i\phi(\tau,T_w,\tau)]\rangle_{H,\mathrm{TLS}}^{N}\ .\end{aligned} \tag{4}$$

In the case where $x\simeq1$, $x^N=\exp(N\ln x)\simeq\exp[-N(1-x)]$, therefore, Eq. (4) can be approximated as

$$C(\tau,T_w,\tau)=\exp\{-N\langle1-\exp[i\phi(\tau,T_w)]\rangle_{H,\mathrm{TLS}}\}\ . \tag{5}$$

The jumps in a TLS between the two levels occur randomly when excited by phonons. The transition rate R between the two levels is known to be distributed very widely, and the distribution function is believed to have a $1/R$ dependence.[23] When $\tau\ll T_w$, as in our experimental conditions, the main contribution to the hole width is due to those TLS's with $R\ll1/\tau$.

Here we consider a TLS whose energy separation between the upper level 2 and the lower level 1 is E. The probability P_{21} that the TLS is initially at level 2 and is found to be at level 1 after T_w, and the probability of the inverse process P_{12} can be expressed as

$$P_{21}=P[\rho_{22}(0)=1]P[\rho_{11}(T_w)|\rho_{22}(0)=1]\ , \tag{6}$$

$$P_{12}=P[\rho_{11}(0)=1]P[\rho_{22}(T_w)|\rho_{11}(0)=1]\ , \tag{7}$$

where $P[\rho_{11}(T_w)|\rho_{22}(0)=1]$ is the conditional probability of finding the TLS in its lower level at T_w given an initial condition $\rho_{22}(0)=1$, and $P[\rho_{22}(T_w)|\rho_{11}(0)=1]$ is that for the inverse process. The relaxation of the population distribution can be expressed as

$$\rho_{11}(t)-\rho_{11}^0=[\rho_{11}(0)-\rho_{11}^0]\exp(-Rt)\ , \tag{8}$$

$$\rho_{22}(t)-\rho_{22}^0=[\rho_{22}(0)-\rho_{22}^0]\exp(-Rt)\ , \tag{9}$$

where ρ_{11}^0 and ρ_{22}^0 are the population densities in thermal equilibrium. From Eqs. (8) and (9) we get

$$P[\rho_{11}(T_w)|\rho_{22}(0)=1]=\rho_{11}^0[1-\exp(-RT_w)]\ , \tag{10}$$

$$P[\rho_{22}(T_w)|\rho_{11}(0)=1]=\rho_{22}^0[1-\exp(-RT_w)]\ , \tag{11}$$

Therefore, when the TLS is in thermal equilibrium, Eqs. (6) and (7) become

$$\begin{aligned}P_{21}=P_{12}&=\rho_{11}^0\rho_{22}^0[1-\exp(-RT_w)]\\&=\tfrac{1}{4}\operatorname{sech}^2(E/2kT)[1-\exp(-RT_w)]\ ,\end{aligned} \tag{12}$$

where k is Boltzmann's constant, and T is the temperature. From Eqs. (3) and (12), we get

$$\begin{aligned}\langle1-\exp[i\phi(\tau,T_w)]\rangle_H&=P_{21}[1-\exp(2i\Delta\omega\tau)]\\&\quad+P_{12}[1-\exp(-2i\Delta\omega\tau)]\\&=\sin^2(\Delta\omega\tau)\operatorname{sech}^2(E/2kT)\\&\quad\times[1-\exp(-RT_w)]\ .\end{aligned} \tag{13}$$

Using Eqs. (5) and (13), $C(\tau,T_w,\tau)$ can be written as

$$C(\tau,T_w,\tau)=\exp\{-N\langle\sin^2(\Delta\omega\tau)\operatorname{sech}^2(E/2kT)[1-\exp(-RT_w)]\rangle_{\mathrm{TLS}}\}\ , \tag{14}$$

which was previously obtained by Bai and Fayer.[23]

Next we need to average over TLS's, where the TLS average means the average over the distance from the guest chromophore, the energy splitting E, and the relaxation rate R. In the organic glass host there exist a large number of voids of various sizes, and it has been pointed out that the polymer chains in some of these organic glasses may form a fractal structure.[25–28] If the TLS's

are somewhere along the polymer chain, it is reasonable to assume that the spatial distribution of the TLS's may also form a fractal structure. Therefore, we assume that the TLS's in the glass host are spatially distributed like a fractal with a fractal dimension D. Then the number of TLS's $N(r)$ within a distance r around a chromophore is expressed as

$$N(r)=\kappa r^{D} , \tag{15}$$

where κ is a constant. The distribution of TLS's is given by

$$P(r)dr=dN(r)/N=(\kappa D/N)r^{D-1}dr . \tag{16}$$

If the interaction between the chromophore and the TLS is a dipole-dipole type interaction, the jump of a TLS at a distance r causes a shift $\Delta\omega(r)$ in the chromophore transition frequency as

$$\Delta\omega(r)=\eta/r^{3} , \tag{17}$$

where η is a constant. Substituting Eq. (17) into Eq. (14), and averaging over r using Eq. (16), we get

$$C(\tau,T_w,\tau)=\exp\{-\tau^{D/3}Z\langle \operatorname{sech}^2(E/2kT)[1-\exp(-RT_w)]\rangle_{E,R}\} , \tag{18}$$

where Z is a constant given as

$$Z=\frac{\kappa D}{3}\eta^{D/3}\int_0^{\infty} x^{-(1+D/3)}\sin^2 x\,dx . \tag{19}$$

If we assume a flat distribution on E, the average of Eq. (18) over E gives

$$\langle \operatorname{sech}^2(E/2kT)[1-\exp(-RT_w)]\rangle_E \propto \int_0^{\infty} dE \operatorname{sech}^2(E/2kT) \propto T . \tag{20}$$

Therefore, the stimulated photon-echo decay function $C(\tau,T_w,\tau)$ becomes

$$C(\tau,T_w,\tau)=\exp(-cT\tau^{D/3}) , \tag{21}$$

where c is a positive constant, T is the temperature, and D is the fractal dimension of the glass host. These results, Eqs. (1) and (21), indicate that, if the fractal dimension D is not 3 ($D=3$ corresponds to a spatially uniform distribution of TLS's), the stimulated photon-echo decay curve is not exponential, and the hole shape is not Lorentzian. Moreover, from Eq. (21) we can derive a temperature dependence of the hole width Γ_{hole} (FWHM) as

$$\Gamma_{\text{hole}} \propto T^{3/D} . \tag{22}$$

III. EXPERIMENTAL AND DISCUSSION

A. Persistent-hole burning in ionic chromophore-doped organic glass

The spatial structure may differ significantly between organic glasses made of long-chained polymers and those made of small monomers. In order to compare the two cases, we first selected two glass hosts, polyvinyl alcohol and ethanol. EtOH is the basic component of PVA, and the degree of polymerization of PVA used was 2000. We selected these two glass hosts, PVA and EtOH, in order to minimize the effects other than the degree of the polymerization. We believe that if the glass is made of long-chained polymer, the size of the voids is distributed in a wide range, and the fractal dimension becomes considerably smaller than 3. On the other hand, if the glass is made of small monomer, the size of the voids is small, and so the fractal dimension should be close to 3.

The chromophore-doped polymer films were made as follows: both the organic dye and PVA were dissolved in water (~60 °C), cast on a glass plate, and dried for several days. The thickness of the film was about 100μm. On the other hand, the chromophore-doped monomer glasses were made by rapidly cooling (~5 K/sec) the solution of the organic dye in EtOH in a glass cell of 1 mm thickness.

The absorption spectra of 1,3,3,1',3',3'-hexamethyl-2-2'-indotricarbocyanine iodide embedded in PVA (HITC:PVA), HITC:EtOH, (Oxazine 1):PVA, and (Oxazine 1):EtOH are shown in Fig. 1. The interesting point in Fig. 1 is that, in both the chromophores, the inhomogeneous width is larger in the polymeric glass than in the monomeric glass. This is consistent with the fact that the distribution of the void sizes of the polymeric glass is considerably broader than that of the monomeric glass.

It is known that in organic glass systems, there exist various types of mechanical rearrangement processes whose time constants vary in a wide range. Therefore, the observation of the hole shape in real time is essential in studying the dynamics in these systems.

The wavelength of a single-mode diode laser can be scanned rapidly by changing its injection current. By using the current sweep of a diode laser, we observed the persistent-hole shape from about 15 msec after burning.[29] Figure 2 shows the persistent-hole shapes observed at 15 msec after burning. The samples were kept at 1.6 K for HITC and 1.7 K for Oxazine 1, in an immersion-type cryostat. Since it is important to minimize the hole shape deformation by saturation or heating, the hole depths burnt were small and were about 3% of the initial absorption. For HITC, we used a MITSUBISHI:ML4402 diode laser which oscillates at 773 nm, and the burn intensity and the burn duration

were 150 μW/cm^2 and 10 msec, respectively. The probing was made by sweeping the wavelength by 1 cm^{-1} in 15 msec at the intensity of 15 μW/cm^2. On the other hand, for Oxazine 1, we used a TOSHIBA:TOLD9215 diode laser which oscillates at 673 nm, and the burn intensity and the burn duration were 600 μW/cm^2 and 15 msec, respectively. The probing beam wavelength was swept by 0.9 cm^{-1} in 15 msec at the intensity of 30 μW/cm^2. The burn wavelengths are shown by arrows in Fig. 1, and the absorbances at the burn wavelengths are about 1 in all the cases.

In both HITC and Oxazine 1, we found very sharp peaks at the center of the holes in the polymeric glass host PVA, whereas the hole shapes in monomeric glass host EtOH are close to Lorentzians. The theoretical curves $I_H(\omega)$ calculated from Eqs. (1) and (21) are shown by dashed curves in Fig. 2. By best fitting we obtained a fractal dimension $D=2.1-2.3$ for PVA. This is considerably smaller than that of the monomeric glass host EtOH, $D=2.7-2.9$, which is close to 3. In order to make clear the comparison between the observed and the theoretical curves, we consider the Fourier transforms of the hole shapes, i.e., the stimulated photon-echo decay function $C(\tau,T_w,\tau)$. The results are shown in Fig. 3 together with the theoretical lines (dashed lines) representing

$$\ln\{-\ln[\exp(-cT\tau^{D/3})]\}=\frac{D}{3}\ln\tau+\text{const.} \tag{23}$$

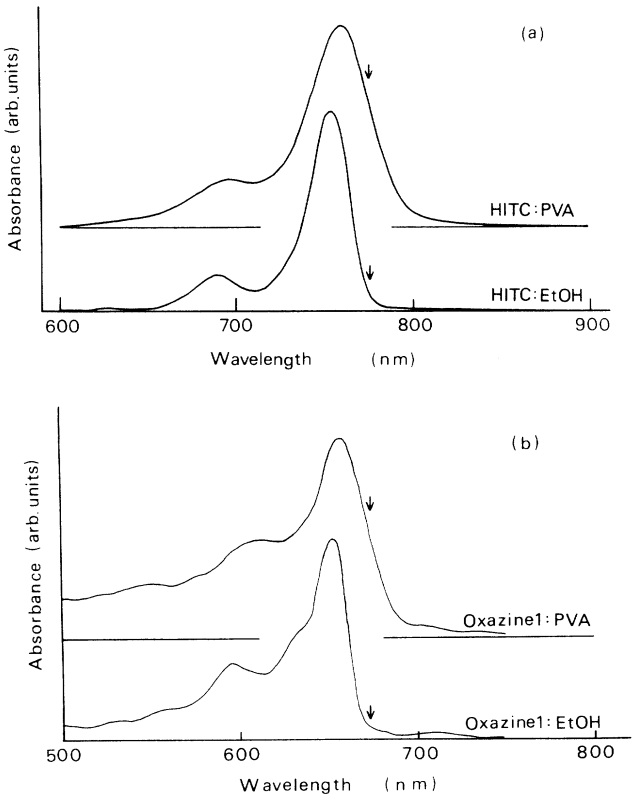

FIG. 1. Absorption spectra of (a) HITC:PVA and HITC:EtOH at 5.4 K and of (b) (Oxazine 1):PVA and (Oxazine 1):EtOH at 1.7 K. The burn wavelengths are shown by arrows.

In Fig. 3 we clearly see differences in the slopes between the lines for PVA and EtOH.

The time evolution of the hole widths Γ_{hole} for (a) HITC at 1.6 K and for (b) Oxazine 1 at 1.7 K are shown in Fig. 4. We see a slight increase of Γ_{hole} by spectral diffusion. A remarkable point in Fig. 4 is that, although

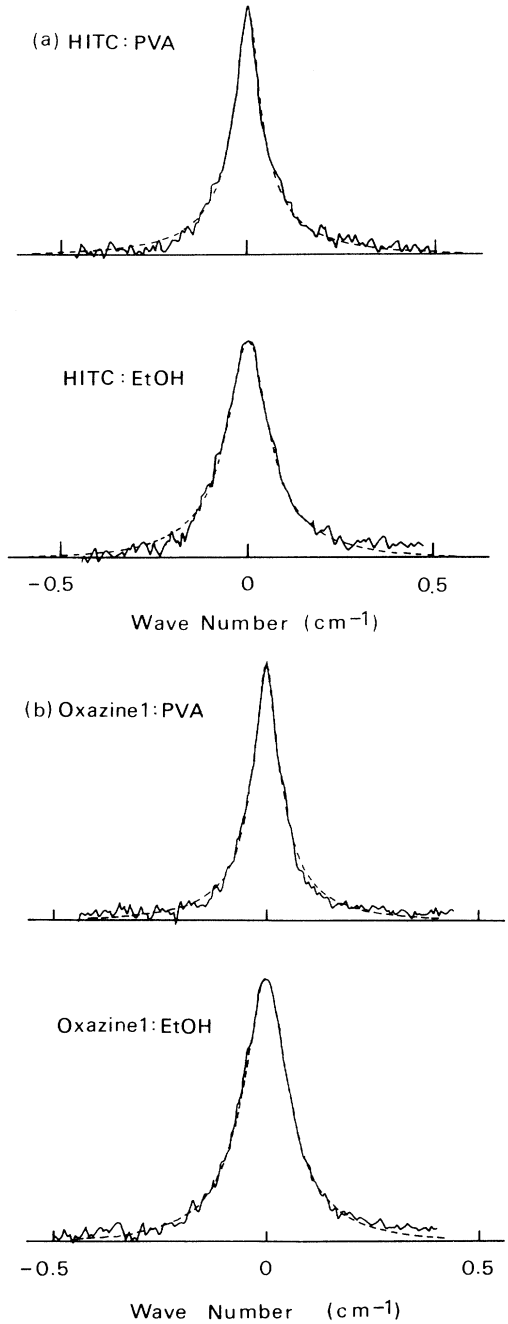

FIG. 2. Persistent-hole shapes of (a) HITC:PVA and HITC:EtOH at 1.6 K and (b) (Oxazine 1):PVA and (Oxazine 1):EtOH at 1.7 K, measured 15 msec after burning, together with the theoretical curves (dashed curves), where $D=2.1$ for HITC:PVA, $D=2.7$ for HITC:EtOH, $D=2.3$ for (Oxazine 1):PVA, and $D=2.9$ for (Oxazine 1):EtOH.

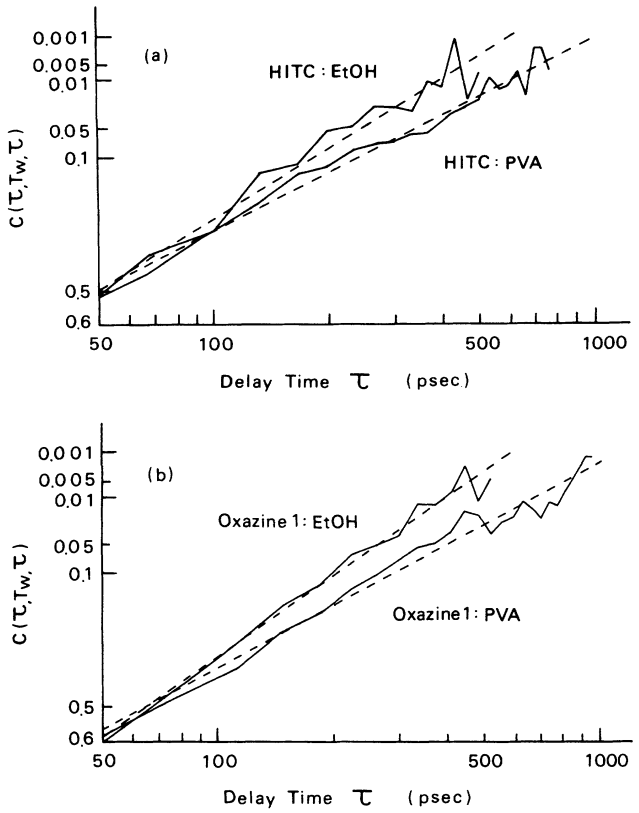

FIG. 3. Fourier transforms of the hole shapes in Fig. 2, $C(\tau,T_w,\tau)$, are plotted as a function of τ for (a) HITC and for (b) Oxazine 1, together with the theoretical lines (dashed lines) representing Eq. (23), where $D=2.1$ for HITC:PVA, $D=2.7$ for HITC:EtOH, $D=2.3$ for (Oxazine 1):PVA, and $D=2.9$ for (Oxazine 1):EtOH.

the inhomogeneous widths for PVA are larger than those for EtOH, as are shown in Fig. 1, the hole widths Γ_{hole} for PVA are smaller than those for EtOH. We believe this is because in the polymeric glass the long-chained polymers intertwine and make a dynamically rigid and stable network which somewhat suppresses the jumps of the TLS's.

B. Persistent hole burning in nonionic chromophore-doped organic glass

The chromophores we tested above are classified as ionic dyes. Since our theory is only concerned with the host structure, it should also be applicable to nonionic materials which exhibit photochemical hole burning. We looked for nonionic chromophores in the wavelength region of near-infrared diode lasers, and found 1,4,8,11,15,18,22,25-octa-*n*-butoxy phthalocyanine (OBPc). The mechanism of the photochemical hole burning of metal free phthalocyanines is known as the tautomerism of the central protons. It is difficult to obtain organic glasses in which phthalocyanines are distributed as a single molecule without stacking. Therefore, the only organic host we could use was polystyrene (PS). Even with this host we paid a lot of attention to avoid the stacking of the phthalocyanine. The sample was prepared as follows: OBPc in chloroform was mixed with PS in acetone. The mixture was cast on a glass plate and rapidly dried on a hot plate within a minute. The film thus made was brittle, but the absorption spectrum was very similar to that of a dilute chloroform solution, which confirmed the absence of stacking. The absorption spectrum at 1.8 K is shown in Fig. 5, the arrow indicates the wavelength where the hole was burnt. The absorbance of the sample film at the burn wavelength was about 1. Here we used a HITACHI:HL7802E diode laser which oscillates at 783.5 nm. The burn intensity and the burn duration were 700 μW/cm^2 and 15 msec, respectively, and the probing was made by sweeping the wavelength by 0.7 cm^{-1} in 15 msec at the intensity of 23 μW/cm^2.

Figure 6 shows the persistent-hole shape measured at 15 msec after burning at 1.8 K. The dashed curve is the theoretical one by Eqs. (1) and (21) with fractal dimension $D=2.4$ obtained by best fitting. For this PS polymeric glass, we also obtained a fractal dimension $D=2.4$ which is considerably smaller than 3. This is more clearly seen by the Fourier transform of the hole shape, the stimulated photon-echo decay function $C(\tau,T_w,\tau)$, as before.

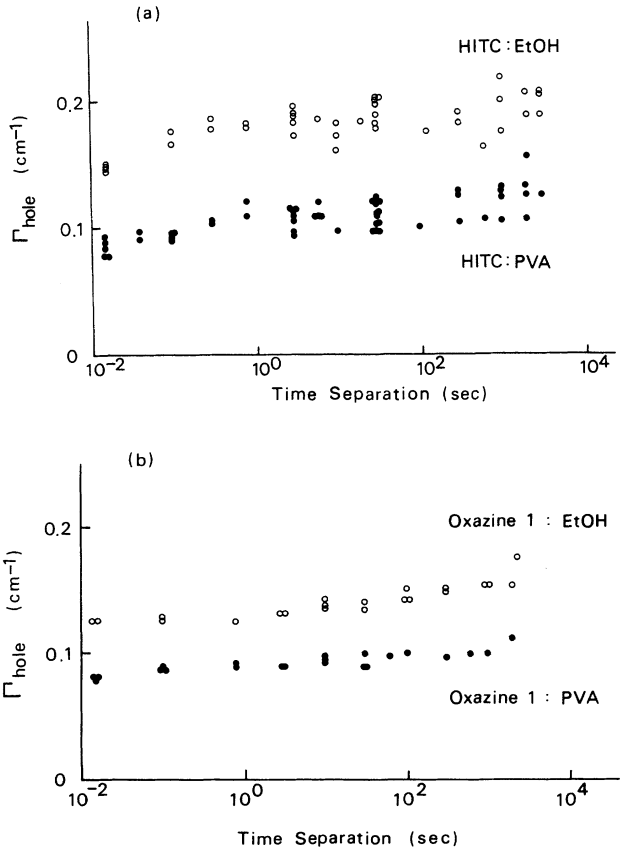

FIG. 4. Time evolution of hole widths Γ_{hole} after burning for (a) HITC at 1.6 K and for (b) Oxazine 1 at 1.7 K, where solid circles and open circles represent those for PVA and EtOH, respectively.

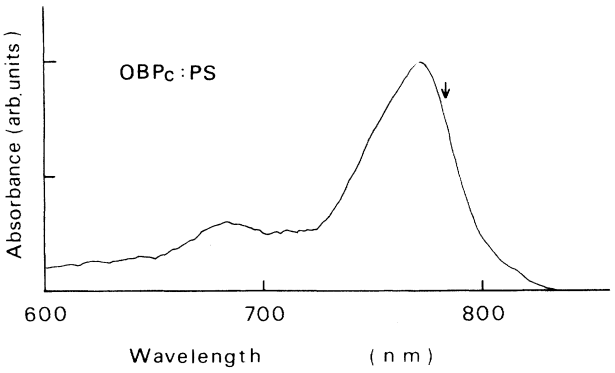

FIG. 5. Absorption spectrum of OBPc:PS at 1.8 K. The burn wavelength is shown by an arrow.

The results are shown in Fig. 7 together with the theoretical line (dashed line) given by Eq. (23) with $D=2.4$. For comparison we showed the line corresponding to $D=3$ by a solid line. In Fig. 7 we clearly see that the fractal dimension D of the polymeric PS glass obtained from the persistent-hole shape is smaller than 3.

Figure 8 shows the time evolution of the hole width Γ_{hole} of OBPc:PS at 1.8 K. We see that the hole width is considerably smaller in OBPc:PS than in the previous samples shown in Fig. 4. The decay rate of the hole depth was also smaller in OBPc:PS. Therefore, we could measure a hole shape at long times after burning with a good signal-to-noise ratio. Figure 9 shows the fractal dimension D obtained from the hole shapes measured at various times after burning. We see that the fractal dimension does not change with time, which is consistent with our theory.

C. Photon echo in chromophore-doped organic glass

In the above we showed that the persistent-hole shape can be explained by the fractal dimension D of the organic glass host. Hence, we think it significant to see this feature directly by the photon-echo decay curve $C(\tau,T_w,\tau)$.

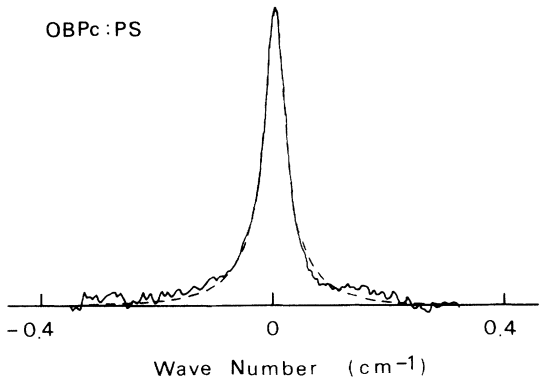

FIG. 6. A typical hole shape of OBPc:PS at 1.8 K, measured 15 msec after burning, together with the theoretical curve (dashed curve), where $D=2.4$.

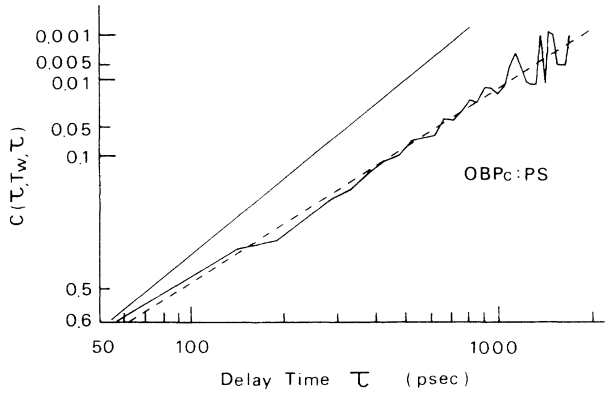

FIG. 7. Fourier transform of the hole shape in Fig. 6, $C(\tau,T_w,\tau)$, is plotted as a function of τ, together with the theoretical line (dashed line) representing Eq. (23), where $D=2.4$. A straight line corresponding to fractal dimension $D=3$ is shown for reference.

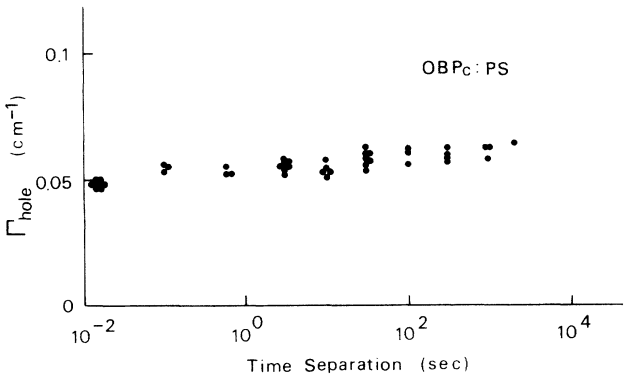

FIG. 8. Time evolution of a hole width Γ_{hole} of OBPc:PS after burning at 1.8 K.

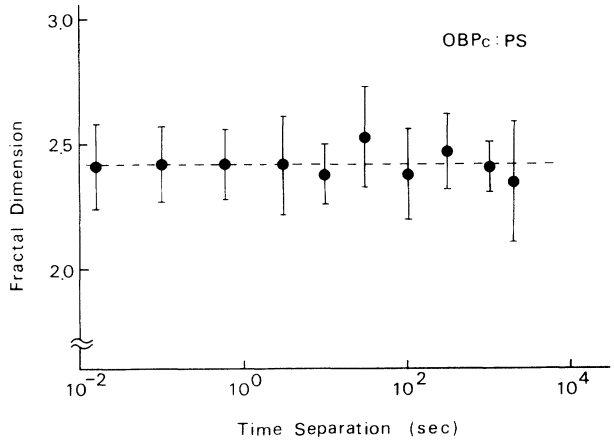

FIG. 9. Time dependence of the fractal dimension D of OBPc:PS after burning at 1.8 K. The dashed line represents the averaged value over the various waiting times from 15 msec to 2000 sec, $D=2.42$.

In the incoherent light accumulated photon echoes, it is possible to obtain a very high time resolution equal to the inverse of the overall spectral width of the excitation light.[30–35] Therefore, as a very handy and stable broadband light source, we used a multimode diode laser SHARP:LT023MD0, which oscillates at 785 nm, and drove it with a rf current at 1 MHz to obtain a smoother spectral profile. The overall spectral width was 3.5 nm, which corresponds to the time resolution of 500 fsec in the photon-echo measurements.

It is well known that in the accumulated photon echoes, it is important to prepare a sample of optically good quality to minimize the scattering of the strong excitation beams by the sample defects which obscure the weak echo signal. But it is quite difficult to obtain a monomeric organic glass of optically good quality. Therefore, in order to suppress the effect of the scattered light, we used the phase-modulation[36] accumulated photon-echo technique, which was recently developed by Saikan, Uchikawa, and Ohsawa.[37]

The schematic diagram is shown in Fig. 10. The excitation beam E_1 was phase modulated at $f=20$ kHz by a piezoelectric actuator. The transmitted beams E_1 and E_2 were detected separately with two photodetectors. The difference signal between the two photodetectors was fed into a lock-in amplifier. The echo signal appears in the $2f$ component of the lock-in detected signal.[37]

The absorption spectra of 3,3′-diethyl-2-2′-thiatricarbocyanine iodide in PVA (DTTC:PVA), and DTTC:EtOH at 5.0 K are shown in Fig. 11. In this case too we see that the inhomogeneous broadening in the polymeric glass is larger than in the monomeric glass.

The echo decay curve was obtained by changing the delay time τ between the first beam E_1 and the second beam E_2. At a fixed delay time τ the echo signal increased with time, which indicates that the signal was induced by the population grating created by persistent-hole burning. At each delay time τ, in order to refill the persistent population grating created previously, we at first irradiated the sample with a diode laser MITSUBISHI:ML4402 for 30 sec, which oscillates at 773 nm, which is shorter than the wavelength of the echo excitation beams. The intensity of the erasing light was 15 mW/cm^2. Next the echo excitation beams were irradiated to the sample for 10 sec, where the intensities were 2.9 mW/cm^2 for DTTC:PVA, and 13 mW/cm^2 for DTTC:EtOH, and then the echo signal was measured. In this accumulated photon-echo measurement, the waiting time T_w extends from 0 to 10 sec, in principle, but the hole widths Γ_{hole} do not change so much with the waiting time T_w from 15 msec to 2×10^3 sec, as are shown in

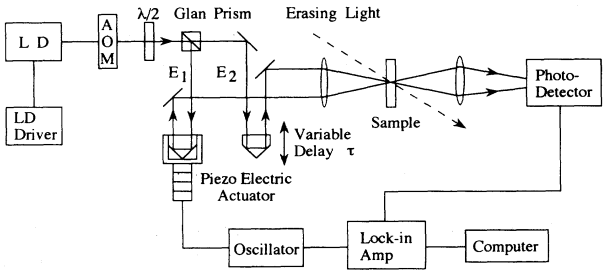

FIG. 10. Schematic diagram of the phase-modulation accumulated photon-echo experiment using a cw multimode diode laser. AOM is an acousto-optic modulator. The excitation beam E_1 was phase modulated at 20 kHz by a piezoelectric actuator. The transmitted beam E_1 and E_2 were detected separately with two photodetectors. The difference signal between the two photodetectors was fed into a lock-in amplifier.

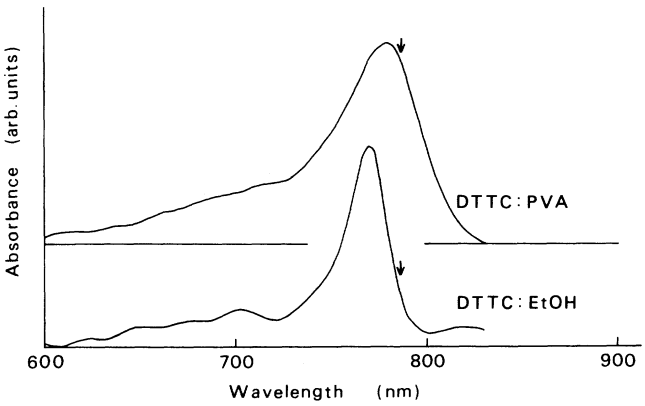

FIG. 11. Absorption spectra of DTTC:PVA and DTTC:EtOH at 5.0 K. The excitation wavelengths of the photon echos are shown by arrows.

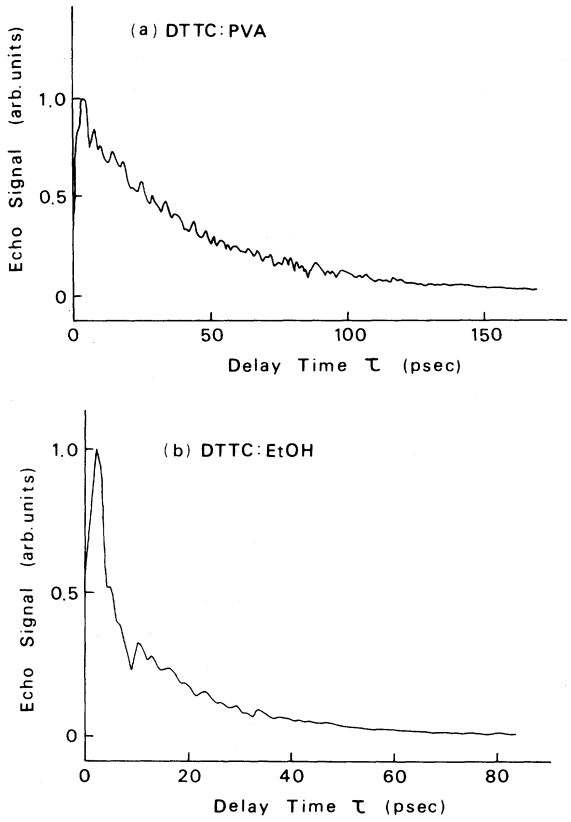

FIG. 12. Photon-echo decay curves of (a) DTTC:PVA and (b) DTTC:EtOH at 5.0 K.

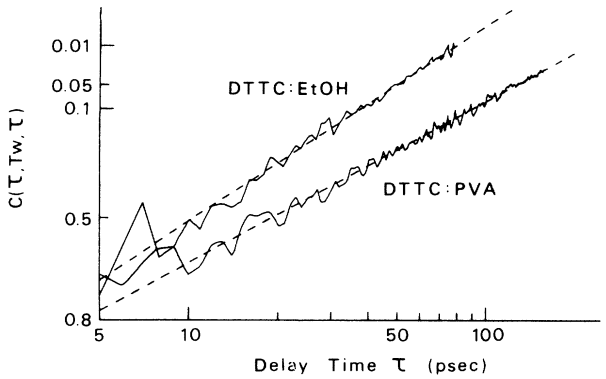

FIG. 13. Photon-echo decay curves $I_{\text{echo}}(\tau)$ in Fig. 12 are plotted as $\ln\{-\ln[I_{\text{echo}}(\tau)]\}$ vs $\ln(\tau)$, together with the theoretical curves (dashed curves) representing Eq. (23), where $D=2.3$ for DTTC:PVA, and $D=2.8$ for DTTC:EtOH.

Figs. 4 and 8. Therefore, we can safely say that the dominant contribution to the echo signal is brought about by the components at $T_w \sim 10$ sec. Thus, we consider the measured echo decay curves $I_{\text{echo}}(\tau)$ to correspond to $C(\tau, T_w, \tau)$ at $T_w \sim 10$ sec. The echo decay curves of DTTC:PVA and DTTC:EtOH at 5.0 K are shown in Fig. 12. In order to make clear the comparison between the measured echo decay curves and the theory, we plotted $\ln\{-\ln[I_{\text{echo}}(\tau)]\}$ (solid line) and

$$\ln\{-\ln[C(\tau, T_w, \tau)]\} = (D/3) \times \ln(\tau) + \text{const}$$

(dashed line) in Fig. 13, where $I_{\text{echo}}(\tau)$ is normalized to 1 as $\tau \to 0$. The dashed lines are obtained by best fitting, $D=2.3$ for DTTC:PVA, and $D=2.8$ for DTTC:EtOH. These values are in good agreement with the values obtained by the persistent-hole shapes as is shown in Fig. 3.

D. Model of organic glass host

In our experiments we found out that between the polymeric glass host and the monomeric glass host there are large differences in the hole shapes and photon-echo decay curves, and in the interrelation between the inhomogeneous and homogeneous widths. In order to explain these features, we propose a simple model for polymeric glass and monomeric glass as is shown in Fig. 14.

In polymeric glasses, the guest chromophore is surrounded by long-chained polymers which intertwine. This structure gives rise to the existence of voids of various sizes, and hence a large inhomogeneous width and a small fractal dimension D. But the dynamical stability of the polymer network yields a small homogeneous width or a small hole width at low temperatures. On the other hand, in monomeric glasses, the guest chromophore is surrounded by small monomers. Therefore, the size of the voids should be considerably smaller and the inhomogeneous width should be also, and the fractal dimension

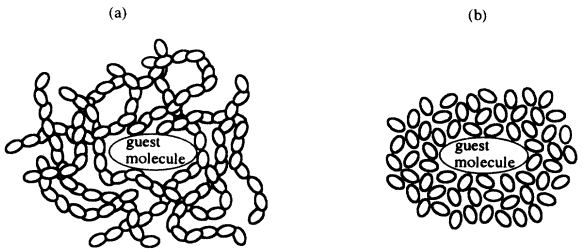

FIG. 14. Model of chromophore-doped organic glass: (a) polymeric glass host, (b) monomeric glass host.

D should be close to 3. But the loose network yields a large homogeneous width or a large hole width.

The key features of the persistent-hole shape in a polymeric glass host with a small fractal dimension D are the sharp peak and the broad wing compared with the Lorentzian shape. In the glass host with a small fractal dimension, the density of the TLS at a short distance from the guest chromophore is larger than that at a longer distance, therefore the jump of the TLS which causes a large frequency shift to the chromophore is relatively more frequent than in the case where the chromophore is embedded in a spatially uniform host ($D=3$). This is the reason for the deviation of the persistent-hole shape from a Lorentzian in a glass host with a low fractal dimension.

IV. CONCLUSION

We proposed that the persistent-hole shape is determined by the fractal dimension of the glass host, and have derived a nonexponential photon-echo decay curve and a non-Lorentzian persistent-hole shape. Values of the host fractal dimension almost independent of the guest chromophore were obtained from the persistent-hole shapes. We also obtained consistent values of host fractal dimension from photon-echo decay curves. The non-Lorentzian persistent-hole shapes were observed in nonionic as well as in ionic guest chromophores and support the proposal presented here. Moreover, our simple model of the spatial structures of polymeric and monomeric glass hosts can consistently explain the obtained hole widths, inhomogeneous widths, and fractal dimensions.

ACKNOWLEDGMENTS

We would like to thank H. Tsukahara of Mitsubishi Paper Mills, LTD. for providing us with OBPc, and T. Hattori and K. M. Abedin for careful readings of the manuscript. This work was supported in part by Grant-in-Aid for Scientific Research 03452050 from the Ministry of Education, Science, and Culture of Japan.

*Present address: Electrotechnical Laboratory, Tsukuba, Ibaraki 305, Japan.

[1]R. C. Zeller and R. O. Pohl, Phys. Rev. B **4**, 2029 (1971).
[2]P. W. Anderson, B.I. Halperin, and C. M. Varma, Philos. Mag. **25**, 1 (1972).
[3]W. A. Phillips, J. Low Temp. Phys. **7**, 351 (1972).
[4]B. M. Kharlamov, R. I. Personov, and L. A. Bykovskaya, Opt. Commun. **12**, 191 (1974).
[5]A. A. Gorokhovskii, R. K. Kaarli, and L. A. Rebane, Pis'ma Zh. Eksp. Teor. Fiz. **20**, 474 (1974) [JETP Lett. **20**, 216 (1974)].
[6]J. M. Hayes and G. J. Small, Chem. Phys. **27**, 151 (1978).
[7]G. J. Small, in *Spectroscopy and Excitation Dynamics of Condensed Molecular Systems,* edited by V. M. Agranovich and R. M. Hochstrasser (North-Holland, Amsterdam 1983), pp. 515–554.
[8]T. L. Reinecke, Solid State Commun. **32**, 1103 (1979).
[9]S. K. Lyo and R. Orbach, Phys. Rev. B **22**, 4223 (1980).
[10]S. K. Lyo, Phys. Rev. Lett. **48**, 688 (1982).
[11]P. Reineker and H. Morawitz, Chem. Phys. Lett. **86**, 359 (1982).
[12]P. Reineker, H. Morawitz, and K. Kassner, Phys. Rev. B **29**, 4546 (1984).
[13]B. Jackson and R. Silbey, Chem. Phys. Lett. **99**, 331 (1983).
[14]J. M. Hayes, R. Jankowiak, and G. J. Small, in *Persistent Spectral Hole-Burning: Science and Applications,* edited by W. E. Moerner (Springer-Verlarg, Berlin, 1988), pp. 153–202.
[15]S. Uemura, K. M. Abedin, M. Okada, and H. Nakatsuka, in Proceedings of the 1991 Spring Meeting of the Physical Society of Japan, 25-X-4, p. 241, edited by the Physical Society of Japan (in Japanese).
[16]S. Uemura, K. M. Abedin, M. Okada, and H. Nakatsuka, J. Phys. Soc. Jpn. **60**, 3557 (1991).
[17]S. Uemura, M. Okada, K. M. Abedin, and H. Nakatsuka, Chem. Phys. Lett. **189**, 193 (1992).
M. D. Fayer, J. Chem. Phys. **88**, 1564 (1988).
[19]S. Saikan, T. Nakabayashi, Y. Kanematsu, and N. Tato, Phys. Rev. B **38**, 7777 (1988).
[20]R. Yano, Y. Matsumoto, T. Tani, and H. Nakatsuka, J. Phys. Soc. Jpn. **58**, 3814 (1989).
[21]P. Hu and L. R. Walker, Phys. Rev. B **18**, 1300 (1978).
[22]R. Maynard, R. Rammal, and R. Suchail, J. Phys. Lett. **41**, L291 (1980).
[23]Y. S. Bai and M. D. Fayer, Phys. Rev. B **39**, 11 066 (1989).
[24]See, for example, S. K. Lyo, in *Optical Spectroscopy of Glasses,* edited by I. Zschokke (Reidel, Dordrecht, 1986), pp. 1–21.
[25]P. J. Flory, *Principles of Polymer Chemistry* (Cornell University Press, Ithaca, N.Y., 1971).
[26]P. G. de Gennes, *Scaling Concepts in Polymer Physics* (Cornell University Press, Ithaca, 1979).
[27]S. Alexander and R. Orbach, J. Phys. Lett. **43**, L625 (1982).
[28]S. Saikan, T. Kishida, Y. Kanematsu, H. Aota, A. Harada, and M. Kamachi, Chem. Phys. Lett. **166**, 358 (1990).
[29]H. Nakatsuka, K. Inouye, S. Uemura, and R. Yano, Chem. Phys. Lett. **171**, 245 (1990).
[30]S. Asaka, H. Nakatsuka, M. Fujiwara, and M. Matsuoka, Phys. Rev. A **29**, 2286 (1984).
[31]N. Morita and T. Yajima, Phys. Rev. A **30**, 2525 (1984).
[32]R. Beach and S. R. Hartmann, Phys. Rev. Lett. **53**, 663 (1984).
[33]S. Asaka, H. Nakatsuka, M. Fujiwara, and M. Matsuoka, J. Phys. Soc. Jpn. **56**, 2007 (1987).
[34]H. Nakatsuka, Y. Matsumoto, K. Inouye, and R. Yano, Opt. Lett. **14**, 633 (1989).
[35]R. Yano, S. Uemura, H. Nakatsuka, and Okada, J. Opt. Soc. Am. B **8**, 1093 (1991).
[36]M. Gehrtz, J. Pinsl, and C. Braeuchle, Appl. Phys. B **43**, 61 (1987).
[37]S. Saikan, K. Uchikawa, and H. Ohsawa, Opt. Lett. **16**, 10 (1991).